CIRCULATION CONTROL STOL AIRCRAFT DESIGN ASPECTS*

John L. Loth

Mechanical and Aerospace Engineering
West Virginia University

Abstract

Since Davidson patented Circulation Control Airfoils in 1960, there have been only two aircraft designed and flown with CC. Designing with CC is complex for the following reasons: the relation between lift increase and blowing momentum is non-linear; for good cruise performance one must change the wing geometry in flight from a round to a sharp trailing edge. The bleed air from the propulsion engines or an auxiliary compressor, must be used efficiently. In designing with CC, the propulsion and control aspects are just as important as aerodynamics. In this paper these design aspects have been examined and linearized equations are presented in order to facilitate a preliminary analysis of the performance potential of CC. The thrust and lift requirements for take-off make the calculated runway lenght very sensitive to the bleed air ratio. Thrust vectoring improves performance and can off-set nose down pitching moments. The choice of blowing jet to free stream velocity ratio determines the efficiency of applying bleed air power.

Introduction

Davidson (1960) patented the Circulation Control concept. The initial application was for cylindrical airfoils. Kind et al (1968) provided experimental data for the elliptical airfoil. The ellipse is desirable for helicopter blade applications because it has some lift generating ability in case of power failure and is structurally rigid. In recent years, it's leading and trailing edges have been modified and camber was added to improve the lift characteristics. More wind tunnel data are available on the basic and modified elliptical shape CC airfoil than all other configurations combined. The elliptical shape with it's maximum thickness near mid-chord has a center of pressure near mid-chord and thus a steeper adverse pressure gradient than conventional airfoils. This thickens the boundary layer upstream of the blowing slot and renders the Coanda turning efficiency very sensitive to geometry, angle of attack, Reynolds number and turbulence level. Various investigators have found significant differences in the lift-to-blowing momentum augmentation ratio for seemingly similar configurations. The non-linearity of this ratio with the blowing coefficient further adds to the complexity of selecting an optimum CC configuration.

* Funded by Lockheed Georgia, Contract No. MDA-53 #108444630

When a CC rounded trailing edge is added to a conventional high lift airfoil, complete with a leading edge modification to prevent separation, it's performance is much more predictable. Such airfoils have their maximum thickness further forward than the ellipse and therefore possess a less steep adverse pressure gradient than the ellipse. The reduced pressure gradient, together with the usually greater chord length and Reynolds number, minimizes the difference in boundary layer shape ahead of the blowing slot for CC modified CTOL wings. Such airfoils can be used for STOL aircraft and provide more comparable lift augmentation ratios and linearity with angle of attack. The greater thickness of a STOL aircraft wing as compared to a helicopter blade, permits incorporating advanced leading edge devices such as Kruger flaps, slats, or drooped leading edges with or without blowing. Large ducts fit inside a STOL wing which permits the power efficient use of blowing air at medium pressure and temperature. An ejector built around the blowing slot can provide boundary layer suction just upstream of the rounded Coanda jet turning surface. For added lift, the chord length may be increased in the CC mode, however the rounded trailing edge must be retracted in order to obtain efficient cruise performance with a sharp trailing edge. The availability of flaps in conjunction with CC is desirable for drag control during descent, adding flexibility and safety in the case of a blowing air failure. Even though the STOL CC airfoil geometry is much more complex than the modified ellipse, it's aerodynamic behavior and linearity is similar to that of the conventional CTOL airfoil. This is evident from the wind tunnel model test data by Englar (1975) on various STOL airfoil configurations. The flight tests on the only two CC STOL aircraft built and tested showed good agreement in lift augmentation ratio and performance, even though these aircraft were significantly different in geometry and wing loading.

Since the CC air mass flow requirements are low they may be provided by a relatively light weight auxiliary turbo-compressor or a compressor driven by shaft power take-off from the thrust engines. In this manner the blowing pressure is independent of the thrust level, thereby simplifying the design and operation with CC. However, the weight, cost, and reliability penalty of an additional compressor makes the use of jet engine bleed air more attractive. The thrust loss associated with compressor bleed air is a complex function of bleed pressure and throttle setting. The bleed mass ratio is one of the most important parameters in determining the effectiveness of CC during the take-off and landing phase. Minimizing the blowing air ducting heat and pressure losses, as well as the throttling loss across the bleed air flow control valve, greatly effects the ratio of blowing thrust generated to engine thrust lost. With CC, the blowing coefficient is in general less than 5% of the lift coefficient, therefore the blowing momentum is a small fraction of the aircraft weight. Most of the momentum is used to energize the boundary layer along the Coanda turning surface. The small fraction remaining in the wall jet after separation is often negligible relative to the take-off thrust coefficient. Even in the high drag landing configuration, the effect of C_μ on the reduction in the drag coefficient can often be ignored.

WVU CC STOL Demonstrator Design Aspects

In 1968, the Office of Naval Research awarded a research contract to West Virginia University to investigate the theoretical and experimental aspects of Circulation Control. This was about the same time that Williams (1970) at NSRDC, started to investigate the performance of elliptical airfoils to be used on a high lift helicopter. As a result, significant improvements were made in the lift-to-blowing momentum augmentation ratio. However, it became apparent that this ratio was very

dependent on the model aspect ratio, slot adjustment mechanism, jet to free stream velocity ratio, tunnel blockage factor, turbulence level and Reynolds number. To eliminate tunnel wall interference and achieve high Reynolds numbers, WVU researchers decided to flight test a CC wing on a light aircraft. The first CC 2-D STOL airfoil built at WVU had a 4 ft chord and incorporated a drooped and blown leading edge. A low pressure blowing slot produced an air jet tangentially to the cylindrical flap hinge. The airfoil could be operated in the blown flap mode or as a CC airfoil after the 15% flap was folded fully forward and flush with the underside of the airfoil. In 1970, this WVU model was tested in the 8 x 10 ft NSRDC tunnel. Even though it performed as anticipated, the following improvements were made. The flap was folded out in the CC mode to increase the chord instead of decreasing it by 15%. The rounded Coanda surface remained stowable in flight, to provide a sharp trailing edge for low drag cruise. A choked flow nozzle was selected for better span-wise blowing uniformity and slot adjustment screws were eliminated. A built in ejector was designed to improve the jet thickness, temperature and Coanda turning of the otherwise supersonic jet. The ejector entrained air provides needed structural cooling and boundary layer suction at the flap hinge. Reducing the boundary layer thickness upstream of the blowing slot greatly improves the Coanda turning. The drooped leading edge was designed by Norio Inumaru, program manager of the Japanese USB QSTOL, and proved to be so effective, that the leading edge blowing could be eliminated. In 1971, the improved CC STOL airfoil (figs. 1 and 2) was tested in the WVU wind tunnel, Loth (1973). At the same time construction was started on the WVU CC STOL Demonstrator Aircraft, using materials from a BEDE 4 home builders kit. A 200 HP GTC 85-72 APU was selected to provide up to 1 kg/sec of air at maximum 2 atm gage, to the CC blowing slot. The blown ailerons could be drooped. Inboard and outboard fences were installed for both aerodynamic and structural reasons (fig. 3). Both chord-wise and span-wise pressure taps were installed on the wing. A sliding blowing air dump valve was installed to provide direct lift control. The DLC valve was actuated by a lever on the throttle quadrant. A splitter valve, linked to the aileron controls, provided optional roll control by differential blowing (fig. 4.)

On April 10, 1974, pilot Shawn Roberts (1974) started 25 hours of flight testing to determine the performance potential and handling qualities of CC. The WVU CC STOL Research program was summarized by Loth and Fanucci (1974). The lift coefficient appeared to increase linearly with angle of attack and with the square root of the blowing coefficient. At high blowing rates, the trim lift coefficient was considerably lower than it was on the CC flap. The loss in lift is due to the download of the stabilator, associated with the large nose down pitching moment. At C_{Lmax}, with thrust power at idle, the CC blowing at $C_\mu = 0.12$ increased the flap lift coefficient from 2.1 to 5.2, or with a lift augmentation ratio: $\Delta C_L/C_\mu = 3.1/0.12 = 25.8$. At the same time the trim C_{Lmax} increased only from 1.98 to 3.8, or with a lift augmentation ratio: $\Delta C_L/C_\mu = 1.82/0.12 = 15.2$ and $C_\mu = 3\%$ of C_{Lmax}. This is considerably lower than the 2-D augmentation ratios obtainable with an elliptical airfoil. CC effectiveness is better described by the proportionality constant $C_B = \Delta C_L/(C_\mu)^{0.5}$, which does not change with C_μ for a given airfoil.

Englar (1978) published wind tunnel data on a three dimensional CC model of a modified A-6A Navy Cruisader. Even though the CC wing configuration was entirely different from the WVU model, the lift augmentation ratio's obtained agree very well. His data shown in figure 5 are nearly linear with angle of attack and with the square root of the blowing coefficient. The solid lines represent an empirical curve fit with $dC_L/d\alpha = 4.74$ and $C_B = 6.1$. In 1979, Englar's efforts resulted in 10 hours of flight testing of a CC modified A-6A Navy Crusader. All the flight test data, Carr

(1986) and wind tunnel model data, appear to have about the same constant of proportionality (C_B), as shown in Table 1.

TABLE 1 COMPARISON OF 3-D STOL WING TEST DATA

SOURCE OF TEST DATA	BLOWING	TAIL-OFF, WING ONLY		TRIMMED AIRCRAFT	
	C_μ	ΔC_L	$C_B = \frac{\Delta C_L}{\sqrt{C_\mu}}$	ΔC_L	$C_B = \frac{\Delta C_L}{\sqrt{C_\mu}}$
1974 WVU CC STOL Aircraft Flight Tests, Loth (1974)					
a) Based on cruise wing area	.12	2.3	6.6	1.8	5.1
b) Based on CC wing area	.10	2.0	6.1	1.5	4.7
1979 Grumman A-6A CC STOL Aircraft Flight Tests, Carr (1986)	0.05			1.3	5.8
	0.025			0.85	5.4
Wind Tunnel A-6A Model Tests Tail-Off, Englar (1978)	0.20	2.75	6.1		
	0.10	2.10	6.6		
	0.05	1.36	6.1		
	0.025	0.90	5.7		

The influence of CC blowing on the lift curve slope ($dC_L/d\alpha$) is negligible. The effect of increasing the wing chord is the CC blowing mode by folding out a flap, is to multiply the lift coefficient by the ratio of the wing area increase. When a flap is used in conjunction with CC blowing, the lift increases as a function of the flap deflection angle (δ_f). This may be estimated from thin airfoil theory as:

$$dC_L/d\delta_f = 2\pi - 2\theta_f + 2 \sin(\theta_f) \tag{1}$$

where the flap hinge locater angle (θ_f) is: $\cos^{-1}(1 - 2\, c_f/c)$. Combining all the factors contributing to the lift coefficient with CC:

$$C_L = \frac{c \text{ (with CC)}}{c \text{ (without)}} \left[\alpha \frac{\partial C_L}{\partial \alpha} + \delta_f \frac{\partial C_L}{\partial \delta_f} + C_B \sqrt{C\mu} \right] \tag{2}$$

Linearized CC Lift Augmentation Ratio.

With a choked flow isentropic CC nozzle, the (2-D) blowing momentum is given by:

$$\dot{m}_j V_j = \rho_j h V_j^2 \quad \text{or} \quad C_\mu = \frac{\dot{m}_j V_j}{q\, c} = \left(\frac{2h}{c}\right) \left[\frac{V_j}{V}\right]^2 \left(\frac{\rho_j}{\rho}\right) \tag{3}$$

For a specified blowing pressure ratio and slot height (h) the momentum is not a function of the temperature (t_j). The reason is that the exit density is proportional to ($1/t_j$), whereas the square of the velocity is proportional to (t_j). In the case of regulated and fixed bleed air flow rate, any heat loss in the duct lowers the nozzle total pressure and therefore the blowing velocity (V_j). Assuming an isentropic

compressor and duct, the jet exit static temperature and density would be identical to the ambient values. In practice, the increase in temperature (t_j) due to compressor inefficiency is approximately off-set by the duct heat and pressure loss, thus the density ratio in the blowing coefficient may often be ignored.

In Figure 6, are wind tunnel test data by Englar (1981), plotted as a function of the lift coefficient versus blowing pressure ratio. The result is highly non-linear. However, when the same data are replotted as a function of velocity ratio (fig. 7), they fall on a straight line! The data appears to fit a single empirical equation with the exception of the data for a very narrow slot operating at high velocity and pressure. The reason may be that the slot deflection under high pressure is more significant at small slot heights. Another explanation may be that at low mass flow rates the expansion becomes more isothermal which would tend to increase the jet velocity, when testing with room temperature compressed air. It is noteworthy that velocity ratios below 1.0 seem to provide no lift augmentation, thus there is a minimum value (C_μ = 2h/c) below which there is no lift augmentation. Such low values, typically below 0.002, are never used and this term becomes negligible at C_μ greater than 0.02. This allows one to linearize the lift augmentation ratio with respect to the square root of the blowing coefficient. In figure 6, the coefficient of proportionality (C_B) equals: 9 for h/c = 0.0003 and 10.9 for h/c = 0.0012. Note that the magnitude of (C_B) for a three dimensional wing is considerably lower and closer to 6 for the conditions shown in Table 1.

Because the engine thrust is reduced when blowing power is extracted, the choice of the blowing velocity to flight velocity ratio, becomes very important. At constant (C_μ), the required blowing power (P_b) decreases in proportion to the reduction in velocity ratio. Then for the linear lift augmentation model, the lift coefficient ratio ($\Delta C_L/P_b$) increases with decreasing velocity ratio, as shown in figure 8. However as (V_j/V) approaches 1.0 the value of ΔC_L reduces to zero, this makes the constant power curve peak at: V_j/V = 2.08. A similar optimum velocity ratio was found with boundary layer energization by tangential blowing to prevent separation in an adverse pressure gradient, Boasson (1985). Note this velocity ratio optimization does not consider blowing air duct characteristics such as: losses, size and weight. When these factors are incorporated the optimum velocity ratio is usually greater than 3.

The effect of duct losses in heat and pressure, are shown in figure 9 in terms of percent blowing momentum recovered at the nozzle. This example is for a typical case where the compressor bleed air is extracted at: 11 atm and 375° C. As can be seen, a 50% loss in air temperature is more detrimental than a 50% duct friction pressure loss. The loss in temperature will be noted by an increase in pressure drop across the valve controlling the bleed air mass flow rate. The reason is that at constant mass flow rate, the loss in temperature results in a reduction of the nozzle total pressure. The reduced nozzle pressure is then transmitted through the subsonic ducting to the control valve.

Thrust Loss Due to CC Blowing Power Extraction

The air power requirements for CC, by blowing over a rounded trailing edge, are greater than for conventional boundary layer control, however less than for any other type of powered lift system such as: the jet flap, augmenter wing, USB, etc. The CC 3-D blowing momentum coefficient, based on the entire wing area rarely exceeds 5% of the lift coefficient, or at C_L = 6 find C_μ < 0.3. Thus even in the

absence of thrust vectoring, the blowing momentum is less than 5% of the weight. For most STOL aircraft this means less than 10% of the thrust. The optimum CC blowing velocity is at least three times higher than the lift-off velocity on take-off and of the same order of magnitude as the cruise velocity. The propulsion system exhaust velocity for a propeller driven aircraft is also of the same order of magnitude as the cruise velocity. Therefore, the jet-kinetic power at the CC nozzle is usually less than 10% of the available thrust power. For jet engine propulsion the exhaust velocity is at least double the cruise speed and the CC jet-kinetic power at the nozzle is usually less than 5% of the thrust power.

An auxiliary compressor for CC blowing can be driven efficiently with a power take-off from propulsion engines driving a propeller. Propeller aircraft suffer a reduction in thrust with forward speed. The power extraction for CC blowing is so low, that the anticipated thrust loss is roughly offset by the associated reduction in lift-off speed, so that lift-off with, or without CC, occurs at about the same thrust to weight ratio! The relative thrust loss due to power take-off can be computed using actuator disk theory and a coefficient of performance (C_p). Without power take-off the static thrust is defined by: (T_o), the induced velocity at the disk by (w_o) and in the wake by ($2\ w_o$). From the change in momentum of the mass flow rate ($\dot{m}$) through disk area (A_d) find:

$$T_o = \dot{m}\ 2\ w_o = 2\ \rho A_d w_o^{\ 2} \tag{4}$$

The ideal power is related to shaft power (P_s) by

$$0.5\ \dot{m}\ (2\ w_o)^2 = 2\ \rho\ A_d w_o^{\ 3} = P_s C_p = T_o w_o \tag{5}$$

$$w_o = \left[\frac{P_s C_p}{2\rho A_d}\right]^{1/3} \sim (P_s)^{1/3} \tag{6a}$$

$$T_o \sim (P_s)^{2/3} \tag{6b}$$

With forward velocity (V), the induced velocity reduces to (w) and the thrust to (T). Assuming constant (P_s) and (C_p) gives:

$$T = \rho\ A_d (V + w)\ (V + 2w) \tag{7a}$$

$$P_s C_p = T\ (V + w) = T_o w_o \tag{7b}$$

solving for (w/V) gives:

$$\frac{w}{V} = 0.5 \sqrt{1 + 4 \left(\frac{T}{T_o}\right)\left(\frac{w_o}{V}\right)^2} \quad -0.5 \tag{8}$$

or the thrust loss with forward speed is:

$$\frac{T}{T_o} = \frac{w_{o/V}}{1 + w/V} = \frac{2\left[\frac{w_o}{V}\right]}{1 + \sqrt{1 + 4\left[\frac{T}{T_o}\right]\left[\frac{w_o}{V}\right]^2}} \tag{9}$$

During take-off and landing at velocities below $3w_o$, [note (w_o) is computed from eq. 6a], the thrust loss can be approximated by:

$$\frac{T}{T_o} = 1 - 0.318\left[\frac{V}{w_o}\right]^{0.678} \tag{10}$$

When the CC blowing power (P_b) is extracted from the propeller shaft by an auxiliary compressor at an overall efficiency (η_b), then the remaining propeller power is reduced to (P_{sb}) and the static induced velocity to (w_{ob}).

$$P_b = 0.5\ \dot{m}_j\ V_j^2 \tag{11}$$

$$P_{sb} = P_s - P_b/\ \eta_b \tag{12}$$

From the dependancy of (w_o) and (T_o) on the available power, the relative change in their magnitude with blowing is found from:

$$\frac{w_{ob}}{w_o} = \left[\frac{P_{sb}}{P_s}\right]^{1/3} \tag{13}$$

$$\frac{T_{ob}}{T_o} = \left[\frac{P_{sb}}{P_s}\right]^{2/3} \tag{14}$$

When the propeller exhaust is vectored, the intake momentum (D_m) is added to the drag and only the outlet momentum is included in the thrust (T_b) or:

$$\frac{D_m}{T_{ob}} = \frac{0.5}{w_{ob}} \tag{15a}$$

$$\frac{T_b}{T_{ob}} = \frac{1 - 0.318\left[\frac{V}{w_{ob}}\right]^{0.678}}{1 - \frac{1}{2w_{ob}}} \tag{15b}$$

The blowing coefficient and CC lift augmentation reduce with increasing compressor pressure ratio and associated velocity (V_j):

$$C_\mu = \frac{T_j}{q\,S} = \frac{2P_b}{q\,V_j S} \tag{16}$$

If flaps are used for speed control then with a constant speed propeller, the compressor rpm, coupled to the propeller shaft, can also remain constant even during landing. This method is lighter and more reliable than using an auxiliary turbo-compressor to obtain constant CC blowing momentum.

For jet aircraft, compressor bleed from either the last, or from an intermediate stage, produces a greater thrust loss than with shaft power extraction in a propeller aircraft. This is due to the loss of mass flow rate through the turbine and nozzle. An additional problem is that jet engine bleed air pressure decreases with RPM or throttle setting. To use this source for CC blowing air, one should be able to maintain a high power setting during approach to landing, which necessitates thrust vectoring. The associated engine thrust loss can be computed from cycle analysis on the T-S diagram. The magnitude of the component efficiencies and the temperature ratio's for the compressor and turbine, determine the thrust loss associated with bleed air and forward speed. For example assume a compressor and turbine efficiency of 80% and 87.5% respectively, a turbine inlet temperature equal five times the ambient temperature and the compressor outlet temperature equals the square root of five times the ambient temperature. This results in a ratio of exhaust velocity to flight velocity given as a function of flight Mach number (M).

$$\frac{V_e}{V} = 2.37\ M \tag{17}$$

The intake density and engine mass flow rate increase by ram compression to about:

$$\frac{\dot{m}}{\dot{m}\ (V = o)} = 1 + 0.5\ M^2 \tag{18}$$

resulting in an exhaust momentum increase with flight Mach number of about:

$$\frac{T}{T_o} = 1 + 0.5\ M^2 \tag{19}$$

The reduced static thrust (T_{ob}) associated with bleed air, can be computed as a function of the bleed mass ratio ($b = \dot{m}_j/\dot{m}$), note: limited to less than 20% for most engines. For example the thrust loss for high pressure bleed with 11 atm at the compressor final stage, is found to be

$$\frac{T_{ob}}{T_o} = (1 - b)^2 \cong (1 - 2b) \tag{20a}$$

With 4 atm at the intermediate compressor stage, the thrust loss is found to be

$$\frac{T_{ob}}{T_o} = (1 - 0.5\ b)\ (1 - b) \cong (1 - 1.5b) \tag{20b}$$

When thrust vectoring is employed the inlet momentum ($\dot{m}\ V = D_m$) is added to the drag, and is about:

$$\frac{D_m}{T_{ob}} = 0.42\ M \tag{21a}$$

The exhaust momentum variation with flight Mach number and bleed air is:

$$\frac{T_b}{T_{ob}} = (1 + 0.5\ M^2)\ (1 - b) \tag{21b}$$

The CC blowing momentum (T_j) obtained with the bleed air, depends on the temperature and pressure losses in the bleed air flow control valve and the ducting. Even when minimal losses are assumed, this results in a ratio of blowing thrust recovered to engine thrust lost of not more than:

$$\frac{T_j}{(T_o - T_{ob})} = 0.4 \text{ at } 11 \text{ atm and } 0.6 \text{ at } 4 \text{ atm} \tag{22}$$

This shows that extracting bleed air at the intermediate compressor stage is more efficient than at the final stage. The cycle analysis can be extended to include the effect of by-pass ratio when a turbofan is used. Experimental jet engine thrust loss data, including the effect of reduced bleed pressure at part throttle, are given by Hemmerly (1977).

Ground Run in Landing and Take-Off

The landing and take-off analysis presented here is based on the treatment by Kohlman (1981). During approach to landing, the descent angle is steep and the required forward component of the thrust is very small. To provide speed control, mechanical drag producing devices are needed unless the thrust can be vectored, for example using Pegasus type nozzles. In equilibrium flight, the minimum decsent velocity can be computed as a function of the available blowing momentum (T_j), from the requirement that the sum of the forces normal and along the direction of flight are zero. For CTOL aircraft with an approach speed equal 1.3 V_{stall} the approach angle of attack is found from

$$\alpha_a = \frac{\alpha_{stall}}{(1.3)^2} \tag{23}$$

For a CC powered STOL aircraft, the same safe approach angle of attack may be specified. If the flap size, deflection angle and effect on C_{Do} are specified then the dynamic pressure (q_a) on approach is found by iteration such that the descent angle (γ_a), isolated from the two equilibrium force equations below, are equal.

$$\gamma_a = \sin^{-1}\left[\frac{q}{(W/S)}\left(C_{Do} + \frac{C_L^2}{\pi e\ AR}\right) + \frac{Dm}{W} - \left[\frac{T_b}{W}\right]\cos\ (\theta_T + \alpha_a)\right] \tag{24}$$

$$\gamma_a = \cos^{-1}\left[\frac{q\ C_L}{(W/S)} + \left[\frac{T_b}{W}\right]\ \sin\ (\theta_T + \alpha_a)\right] \tag{25}$$

The resulting descent angle shall not be too steep, otherwise the pilot's visability is impaired or the vertical component of the approach velocity may exceed 1000 ft/min. If such a problem occurs, then the flap or thrust vector angle must be reduced. An advantage of circulation control over other boundary layer control techniques is that high values of the lift coefficient can be obtained at moderate angles of attack. During a steep descent at an angle (γ_α) greater than the angle of attack, the aircraft attitude will be nose down, providing good pilot visibility. To obtain a flare-out before touch down one must be able to generate extra lift, by either having extra angle of attack or blowing pressure available. If one third of the lift is provided by each: the angle of attack, the CC lift augmentation, and the vectored thrust, then increasing the angle of attack for flare is only one third as effective as it is in a CTOL aircraft! During the optimum performance approach, there is no extra lift available, therefore the flare distance contribution to the landing may be ignored. The FAA specifies that after touch-down the deceleration rate is limited for passenger comfort to dV/dt = -0.5 g. If the deceleration rate is constant then the ground roll (s_q) is directly proportional to the minimum approach dynamic pressure or

$$s_g(\text{landing}) = \frac{q_a}{\rho\left[-\frac{dV}{dt}\right]} \tag{26}$$

For take-off, the above equation shows that the ground run is likely just as sensitive to the minimum lift-off dynamic pressure (q_{lof}) as it is to the acceleration. To minimize the lift-off speed one needs high blowing rates and high thrust angles. However, to maximize acceleration one needs all the obtainable thrust in the horizontal direction. Consequently optimum performance is obtained by delaying CC blowing and thrust vectoring to the moment of lift-off! Such a last minute configuration change increases the pilot's work load and reduces safety. Assuming there are no last minute configuration changes permitted, one finds that the optimum bleed air flow rate and thrust vector angle, become very important parameters in the take-off ground run distance optimization, more so than in the climb distance optimization. During the groundrun, on a low friction, level runway, the ground effect due to CC blowing may be ignored. At the start when q=o find C_μ=∞, and the lift increase due to CC should be ignored till C_μ reduces below 0.3. On the ground, the angle of attack (α_g) is constant prior to rotation and the ground distance is found by integrating the equation for the horizontal acceleration from (q_w) to (q_{lof}). Where (q_w) is the dynamic pressure of the head wind component and (q_{lof}) is the lift-off dynamic pressure. After rotation to (α_{lof}), the sum of the lift and vertical component of the thrust vector equals the weight. The take-off distance (s_g) is:

$$s_g = \frac{1}{\rho g}\int_{q_w}^{q_{lof}} \frac{\left(1-\sqrt{\frac{q_w}{q}}\right)\,dq}{\left(\frac{T_b}{W}\right)\cos(\theta_T+\alpha_g) - f\left(1-\left(\frac{T_b}{W}\right)\sin(\theta_T+\alpha_g)\right) - qC_L/\left(\frac{W}{S}\right)\Big] - qC_D/\left(\frac{W}{S}\right) - \frac{D_m}{W}} \tag{27}$$

Near the end of the ground run, the rotation velocity is reached, and the pilot uses the elevator to increase the angle of attack by at least three degrees per second. Ideally, lift-off is achieved just prior to complete rotation to the maximum safe climb-out angle of attack. This ensures definite lift-off with an upward acceleration. To maintain a safe margin below the stall angle of attack, CTOL aircraft are specified to lift off at 20% above the stall speed or at an angle of attack: α_{lof} = α stall/$(1.2)^2$ = 70% of the stall angle. If the same (α_{lof}) angle of

attack is used on STOL aircraft, with powered lift and thrust vectoring, then the lift-off speed safety margin is less than 20% above the stall speed. When the lift-off angle of attack is specified, the lift-off dynamic pressure can be found from:

$$0 = 1 - \left(\frac{T_b}{W}\right) \sin(\theta_T + \alpha_{lof}) - \frac{q_{lof}}{(W/S)} \left[\alpha_{lof} \frac{\partial C_L}{\partial \alpha} + \delta_f \frac{\partial C_L}{\partial \delta_f} + C_B \sqrt{\frac{(T_j/S)}{q_{lof}}} \right] \quad (28)$$

This is a quadratic equation in $(q_{lof})^{0.5}$ or

$$q_{lof} = \left[\frac{-C_B \sqrt{\left(\frac{T_j}{S}\right)} + \sqrt{C_B^2 \left(\frac{T_j}{S}\right) + 4\left[\left(\frac{W}{S}\right) - \left(\frac{T_b}{S}\right)\sin(\theta_T + \alpha_{lof})\right]\left[\alpha_{lof} \frac{\partial C_L}{\partial \alpha} + \delta_f \frac{\partial C_L}{\partial \delta_f}\right]}}{2\left[\alpha_{lof} \frac{\partial C_L}{\partial \alpha} + \delta_f \frac{\partial C_L}{\partial \delta_f}\right]} \right]^2 \quad (29)$$

Maximum Climb Performance

During the climb period needed to clear an obstacle, the thrust vector angle and the flap angle are not altered for safety reasons. The pilot only modulates the aircraft attitude and thus angle of attack to maximize the rate by which the maximum climb angle is reached. Because of the limited effectiveness of the angle of attack, it should as high as practical, while allowing an assymptotic approach to the maximum climb angle (γ_X) at (α_X). A near optimum performance will be obtained when the angle of attack is reduced in proportion to the available acceleration, but never lower than (α_X).

$$\alpha = \alpha_X + \frac{(\alpha_{lof} - \alpha_x)\left(\frac{dV}{dt}\right)}{\frac{dV}{dt}(\text{at lift-off})} \quad (30)$$

If the climb angle increases sufficiently fast, then the velocity does not overshoot the maximum climb angle value (V_X). In case it does exceed (V_X) the acceleration dV/dt will eventually become negative at which time (α_X) must be held constant. To apply this equation one must first compute the maximum climb angle parameters.

From energy considerations, one may determine the steady state climb angle by equating the excess thrust power to the rate of increase in potential energy or

$$[T_b \cos(\theta_T + \alpha) - D - D_m]V = W.RC \quad (31)$$

The maximum climb angle is reached when: $\sin(\gamma) = \left(\frac{RC}{V}\right)$ is maximum or

$$\sin(\gamma_X) = \left[\left(\frac{T_b}{W}\right) \cos(\theta_T + \alpha) - \left(\frac{D}{W}\right) - \left(\frac{D_m}{W}\right)\right]_{max.} \quad (32)$$

When the engine thrust components are independent of flight speed, then the maximum climb angle occurs when the drag is minimum or $(C_{Do} = C_{Di})$. Without

powered lift (C_L) is proportional to (α) and the induced drag coefficient is related to the lift coefficient squared. Then (C_{Lx}) and (α_x) are found from

$$C_{Lx} = \sqrt{C_{Di}\ \pi\ e\ AR} \quad = \sqrt{C_{Do}\ \pi\ e\ AR} \tag{33}$$

$$\alpha_x = \frac{C_{Lx} - \delta_f \dfrac{\partial C_L}{\partial \delta_f}}{\dfrac{\partial C_L}{\partial \alpha}} \tag{34}$$

The maximum climb angle dynamic pressure (q_x) is obtained when the sum of the forces normal to V are zero or

$$\cos^2(\gamma_x) = \left[\left(\frac{T_b}{W}\right) \sin\ (\theta_T + \alpha_x) + q_x\ C_{Lx} / \left(\frac{W}{S}\right)\right]^2 \tag{35}$$

Eliminate (γ_x) from Eq. 32 and 35 by using:

$$\cos^2(\gamma_x) = 1 - \sin^2(\gamma_x) = 1 - \left[\frac{T_b}{W} \sin\ (\theta_T + \alpha_x) - 2C_{Do} q_x / \left(\frac{W}{S}\right) - \frac{D_m}{W}\right]^2 \tag{36}$$

This gives a quadratic equation from which (q_x) can be determined. In general, the thrust is not constant and the maximum climb angle values are found by iteration. For steady state climb, the sum of the forces parallel and normal to the direction of flight equal zero, they are respectively:

$$o = \left(\frac{T_b}{W}\right) \cos\ (\theta_T + \alpha) - \frac{D}{W} - \frac{Dm}{W} - \sin\ (\gamma) \tag{37}$$

$$o = \left(\frac{T_b}{W}\right) \sin\ (\theta_T + \alpha) + \frac{L}{W} - \cos\ (\gamma) \tag{38}$$

At any flight speed, the tangent of the climb angle is obtained from their ratio.

$$\tan\ (\gamma) = \frac{\left(\dfrac{T_b}{W}\right) \cos\ (\theta_T + \alpha) - \dfrac{D}{W} - \dfrac{D_m}{W}}{\left(\dfrac{T_b}{W}\right) \sin\ (\theta_T + \alpha) + \left(\dfrac{L}{W}\right)} \tag{39}$$

The maximum climb angle (γ_x) is a function of angle of attack and found by iteration. Starting with $V = V_{lof}$ and $\alpha = \alpha_{lof}$, decrease (α) until $\tan(\gamma)$ reaches a peak value, which represents a steady state climb. Higher climb angles can be found at higher velocities. Increment (V) and reduce (α) by a small amount until the next steady state value for $\tan(\gamma)$ is reached. This process is continued until the steady state value of $\tan(\gamma)$ reaches a maximum, at which time the desired magnitudes of: V_x, α_x and γ_x have been obtained. The unsteady climb performance computation can now be performed.

Starting at lift-off with $V=V_{lof}$ and $\gamma = o$, integrate the equations of motion until an obstacle of specified height has been cleared. The corresponding climb distance (s_c) must be added to the ground run to determine the total take-off distance. With powered lift, all the aerodynamic coefficients such as: lift, blowing momentum and drag are functions of the dynamic pressure (q). The second most important parameter is the climb angle (γ) or time (t). In general only time is a montonic increasing variable and both acceleration component equations ($\parallel$ and $\perp$ to V) must be incorporated in the numerical integration.

$$\frac{dV}{dt} = g \left[\left(\frac{T_b}{W}\right) \cos(\theta_T + \alpha) - \frac{D}{W} - \frac{D_m}{W} - \sin(\gamma)\right] \tag{40}$$

$$\frac{V d\gamma}{dt} = g \left[\left(\frac{T_b}{W}\right) \sin(\theta_T + \alpha) + \frac{L}{W} - \cos(\gamma)\right] \tag{41}$$

The initial value of the derivative ($d\gamma/dt$) is zero if the climb-out is started with $\alpha = \alpha_{lof}$. However in practice the lift-off rotation may be continued to start climbing with (α) slightly greater than (α_{lof}) and ($d\gamma/dt$) finite. If (γ) increases monotonically, then the ratio's of the two acceleration equations may be used to eliminate the variable (dt) the result being a single equation in terms of ($d\gamma/dq$):

$$\frac{d\gamma}{dq} = \frac{\left(\frac{T_b}{W}\right) \sin(\theta_T + \alpha) + \frac{L}{W} - \cos(\gamma)}{2q\left[\left(\frac{T_b}{W}\right) \cos(\theta_T + \alpha) - \frac{D}{W} - \frac{D_m}{W} - \sin(\gamma)\right]} \tag{42}$$

This technique is not applicable to a ski-jump take-off where (γ) first decreases before it increases. Then one must integrate Eqs. 40 and 41 with respect to time. Once the values of the (V), (γ) are found at each time increment, the corresponding horizontal and vertical distance increments are found from:

$$dx = dt\ [V \cos(\gamma)]\ \text{(average)} \tag{43}$$

$$dy = dt\ [V \sin(\gamma)]\ \text{(average)} \tag{44}$$

The integration can be terminated as soon as the vertical distance (y) exceeds the obstacle height (h). The corresponding climb-distance is found by interpolation:

$$s_c = x - \left(\frac{dx}{dy}\right)(y - h) \tag{45}$$

and the total take-off distance is

$$s = s_c + s_g \tag{46}$$

Because the dynamic pressure (q) is inversely proportional to the wing loading (W/S), all the distance dimensions can be computed as the ratio s/(W/S), when the the obstacle height is specified in terms of h/(W/S). The velocities are then found in terms of $V/(W/S)0.5$.

For CTOL aircraft the maximum climb angle and the difference between V_X and V_{lof} are small. In such a case the steady state climb is reached quickly and prior to clearing the obstacle. For STOL aircraft, the maximum climb angle as well as the difference between V_X and V_{lof} are large as shown in fig. 10. In that case, the obstacle may be cleared prior to reaching the steady state conditions. Due to the limited rate of increase in the climb angle it is possible to overshoot (V_X) prior to reaching the steady state climb angle (γ_X). When the pilot modulates the angle of attack as suggested in eq. 30, then the time required to reach the steady state climb angle (γ_X) is minimal. Because (γ_X) decreases with bleed air, it is advisable to decrease the blowing rate gradually during climb-out.

Example of a Take-Off Performance

To determine the minimum runway length for a CC STOL aircraft, the designer must compare the performance over a wide range of bleed air mass flow ratio's and thrust vector angles. The associated lift and blowing coefficients vary drastically and should not be used as design input variables. Suitable input parameters are: take-off thrust to weight ratio, thrust vector angle, blowing momentum as a function of bleed air mass ratio, thrust loss as a function of blowing momentum, and lift proportionality constant (C_B). All other input parameters are similar to those needed for a CTOL aircraft. A sample calculation was performed for an aircraft with the following characteristics:

$T_O/W = 0.5$, (e AR) = 5, $\partial C_L/\partial\alpha = 4.74$, $C_B = 5.6$ $\alpha_g = 3°$, $\alpha_{lof} = 11°$, $\delta_f = 0$,

blowing air supplied at 11 atm, and duct momentum loss 20%. The distances for both the ground roll and the climb distance are given as a function of the wing loading (W/S). This requires the obstacle height to be specified in the same units. Here (h = 0.5), this means (h = 35 ft) for a wing loading of 70 psf. The ground run distance is shown in fig. 11 to reach a minimum at 5.5% bleed air and a thrust vector angle of 24 degrees. The minimum ground distance in ft is 15.3 times the wing loading in psf. This is less than half the distance required without CC or thrust vectoring. At this low thrust to weight ratio the effect of thrust vectoring by itself is about 20%. The loss of thrust and acceleration associated with high bleed ratios and thrust vectoring are clearly noticeable. In fig. 12, both the climb distance to clear an obstacle and the total take-off distance are shown. The penalty of not using the optimum bleed air ratio and thrust vector angle is not as critical for the climb distance as for the ground distance. This would be different if the bleed air extraction were delayed till the moment of lift-off. The usual obstacle height is 15 meter or 50 ft. If those distances were used, the climb distance would be closer to the ground distance. The trimmed lift coefficient, shown in fig. 13 varies widely with blowing rate from below 1.0 to above 4.0 and for the minimum take-off distance, it is significantly below the maximum obtainable value. The corresponding blowing coefficient varies with the lift-off dynamic pressure as shown in fig. 14. Like the lift coefficient, it varies over a wide range of values. Practical values are limited to below 0.3, above that value the lift augmentation ratio equal $\Delta CL/(C_\mu)^{0.5}$ becomes less effective.

Conclusions

Designing with CC requires a good insight in CC airfoil aerodynamics, the relation between engine thrust loss as a function of blowing air generation and the lift loss associated with trimming the pitching moments. The large number of design variables involved, necessitates numerous performance calculations were each parameter is varied over a wide range. The linear equations presented in this paper facilitate such an analysis. The thrust loss equations should be modified in accordance with the characteristics of the engine under consideration. Because cost, weight, simplicity and reliability are over-riding factors in the optimization process the minimum achievable take-off and landing distances may not represent the optimum design. The finally selected percent bleed air and duct size are probably lower than those corresponding to the minimum runway length. The partial derivatives of these parameters, such as (ds/db), should be plotted as a function of the high lift system cost or weight, to arrive at an optimum design.

In a comparitive study with other high lift techniques one must realize that even though the power efficiency of CC is very attractive, the magnitude of the locally obtainable lift coefficient, is less than six. Desirable flying aspects are good pilot visability and effective DLC. Undesirable characteristics are sudden wing stall, and required in flight stowing of the rounded trailing edge. From the WVU CC flight test, it was found that drag, with the forward folding CC flap in the downward position, was so large that at full throttle, the sink rate was 1000 ft/min. Because the flap folding maneuver could be completed within four seconds, the change in speed and pitch attitude was acceptable.

An improvement in the stowable flap design was recently patented, see figure 15. Here an independently operating Fowler flap is equipped with a CC rounded trailing edge, when needed. Safety and descent control are enhanced by the availability of conventional flaps in conjunction with CC. A separate air duct, which doubles as a rounded Coanda surface, can be swung in position, like an agricultural airplane spray bar. The available internal ejector suction provides the attachment force between the flap trailing edge and the CC air duct. The duct pivot point can be positioned anywhere to accommodate duct stowing at an optimum location in the wing. The drag associated with stowing only the blowing duct, is much lower than with a forward folding flap.

References

1. Boasson, M., Loth, J.L., "Combination of Suction and Tangential Blowing in Boundary Layer Control" 27th Israel Conf. on Aviation and Astronautics, Feb. 1985.

2. Carr, J.E. "Blended Blown Flaps and Vectored Trust for Low Speed Flight", J. Aircraft, Vol. 23, No. 1 1986 p. 26-31.

3. Davidson, I.M., "Aerofoil Boundary-Layer Control System", British Patent No. 913754, 1960.

4. Englar, R.J., "Circulation Control for High Lift and Drag Generation on STOL Aircraft. Journal of Aircraft. Vol. 12, No. 5, May 1975, pp. 457-463.

5. Englar, R.J., Trobaugh, L.A. and Hemmerly, R.A., "STOL Potential of the Circulation Control Wing for High-Performance Aircraft", J. of Aircraft, Vol. 15, No. 3, March 1978, pp. 175-181.

6. Englar, R.J., "Low-Speed Aerodynamic Characteristics of a Small, Fixed Trailing Edge Circulation Control Wing Configuration Fitted to a Supercritical Airfoil. DTNSRDC/ASED-81/08, March 1981.

7. Hemmerly, R.A., "An Investigation of the Performance of a J52-P-8A Engine Operating Under the Influence of High Bleed Flow Extraction Rates", DT NSRDC ASED-387, August 1977.

8. Kind, R.J. and Maull, D.J., "An Experimental Investigation of a Low-Speed Circulation Controlled Aerofoil", Aeronautical Quarterly, Vol. XIX, May 10, 1968, pp. 170-182.

9. Kohlman, D.L. "VSTOL Airplanes", Iowa State U. Press, 1981.

10. Loth, J.L., "Some Aspects of STOL Aircraft Aerodynamics", SAE Paper No. 730328, Business Aircraft Meeting, April 1973.

11. Loth, J.L., Fanucci, J.B., Roberts, S.C., "Flight Performance of a Circulation Controlled STOL Aircraft", Journal of Aircraft, Vol. 13, No. 3, March 1976, pp. 169-173, also AIAA Paper 74-994, August 1974.

12. Loth, J.L., Boasson, M., "Circulation Controlled STOL Wing Optimization," J. Aircraft, Vol. 21, No. 2, 1984, pp 128-134.

13. Roberts, S.C., "WVU Circulation Controlled STOL Aircraft Flight Tests", WVU Aerospace Technical Report No. 42, July 1974.

14. Williams, R.M. and Howe, H.J., "Two-Dimensional Subsonic Wind Tunnel Tests on a 20 Percent Thick, 5 Percent Combined Circulation Control Airfoil. NSRDC TECH. Note AL-176 (AD877-764) 1970.

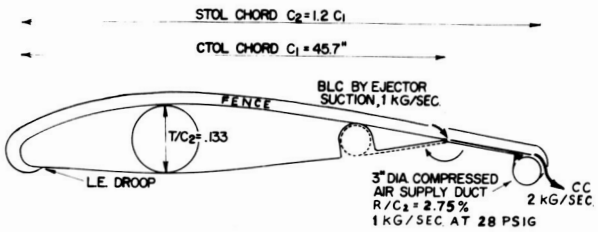

Figure 1 - CC airfoil used on the WVU CC Demonstrator STOL aircraft.

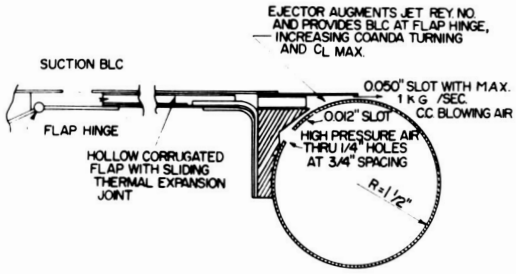

Figure 2 - Hollow flap of the WVU CC wing with supersonic jet ejector.

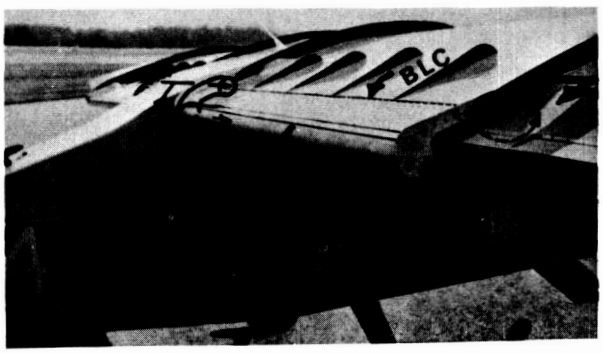

Figure 3 - WVU STOL aircraft with aerodynamic and structural fences needed to transfer loads past the CC duct stowing cavity.

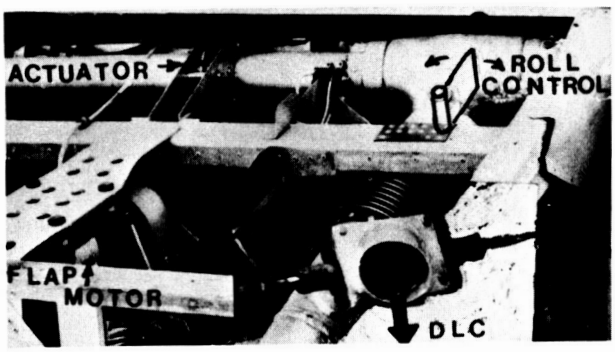

Figure 4 - CC air supply with DLC sliding air dump valve and aileron linked splitter vane for roll control by differential blowing.

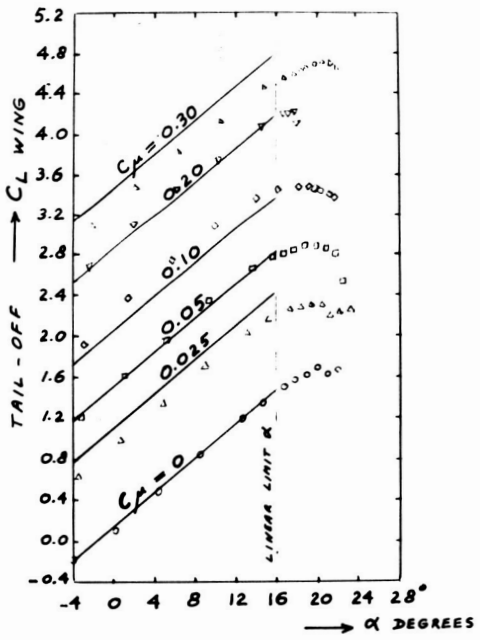

CURVE FIT: $C_{L_{WING}} = 4.74(\alpha + 0.028 \text{ RADIAN}) + 6.1\sqrt{C_\mu}$

Figure 5 - Empirical curve fit with Eq. 2, applied to wind tunnel data on A-6 model with tail-off.

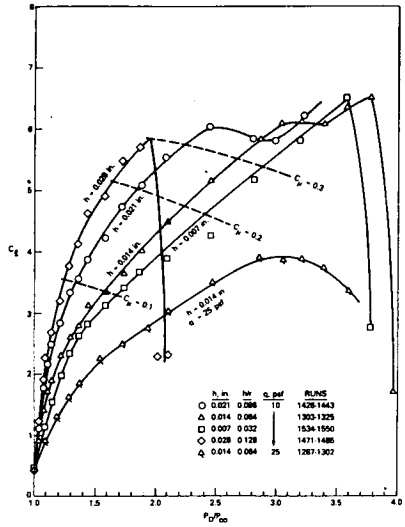

Figure 6 - Non-linear CC airfoil lift versus blowing pressure.

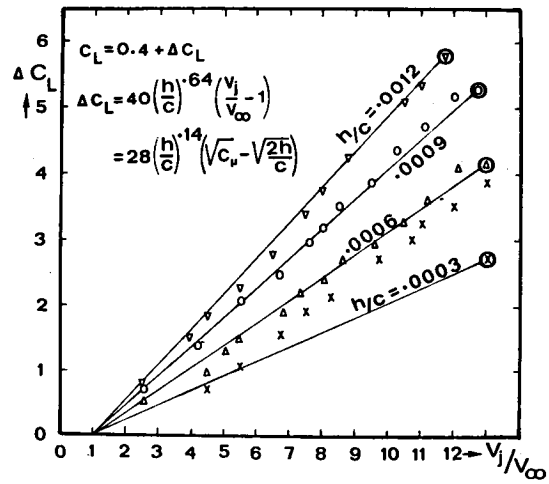

Figure 7 - Linear CC airfoil lift increase versus velocity ratio.

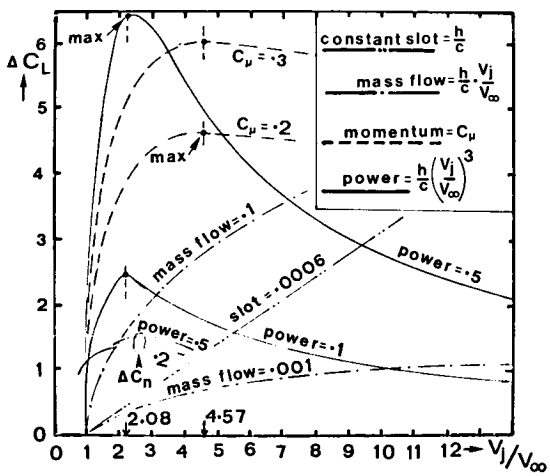

Figure 8 - Effect of velocity ratio on lift increase at constant power.

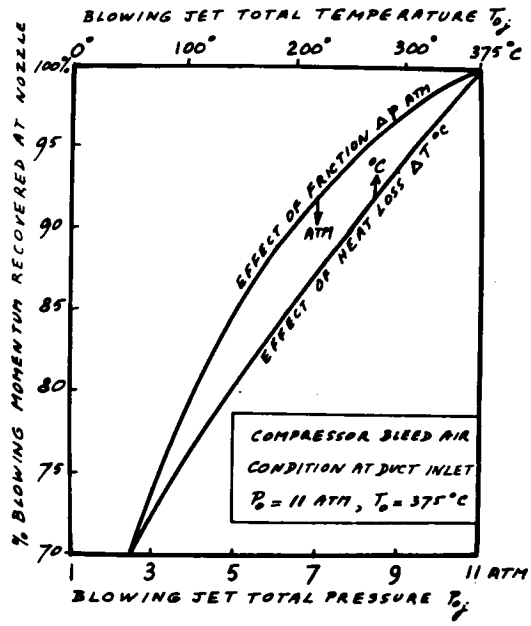

Figure 9 - Example of reduction in blowing momentum due to duct loss.

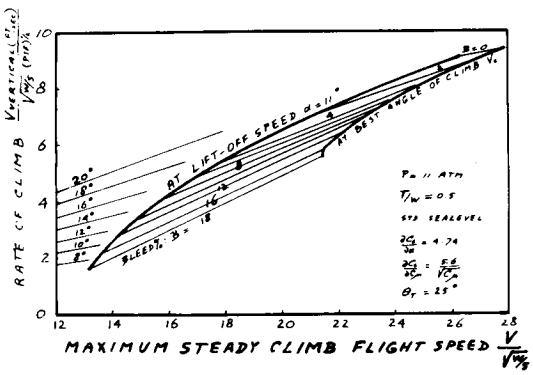

Figure 10 - Reduction in lift-off and best climb angle speed with CC.

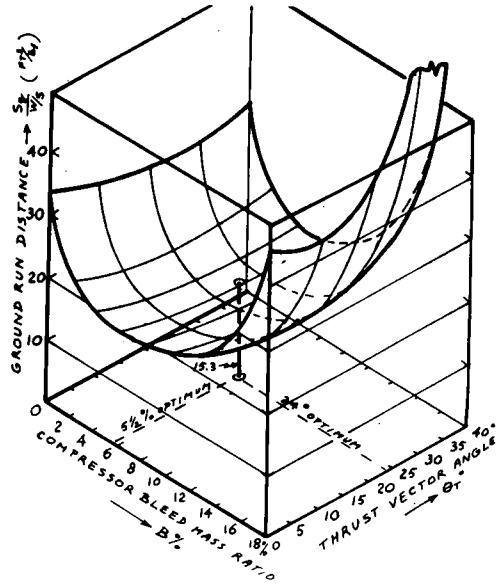

Figure 11 – Example of reduction in take-off ground run with CC.

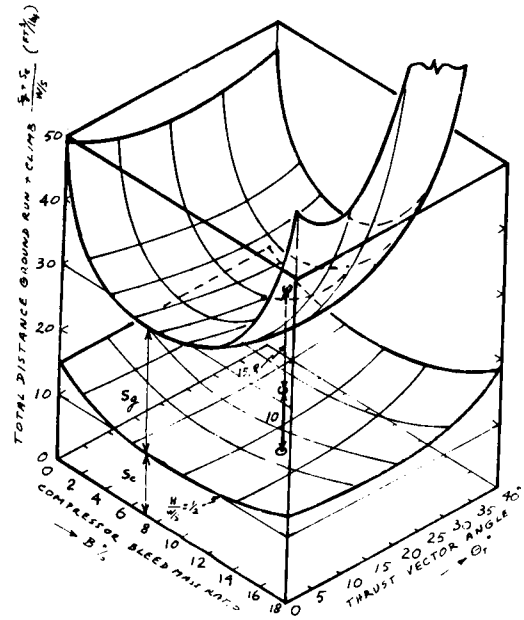

Figure 12 – Example of reduction in climb and ground distance with CC.

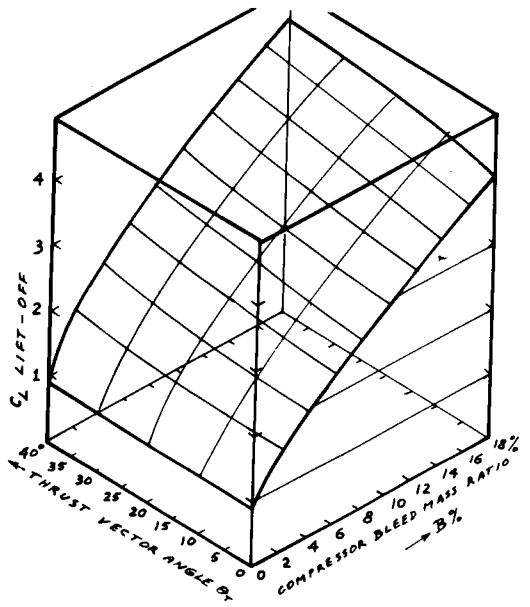

Figure 13 – Example of range in C_L lift-off available with CC.

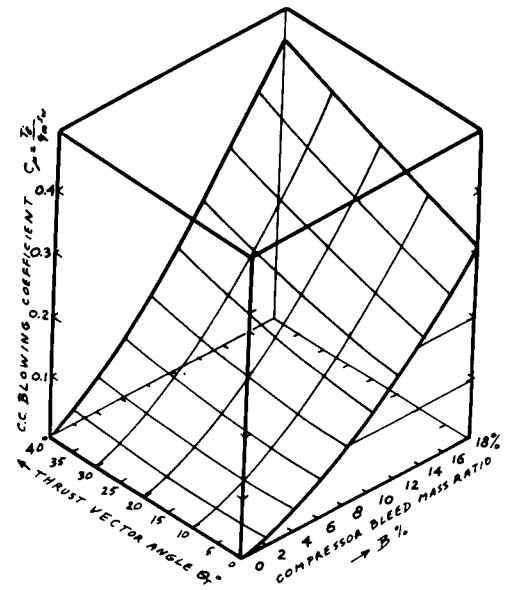

Figure 14 – Example of range in C_μ lift-off available with CC.

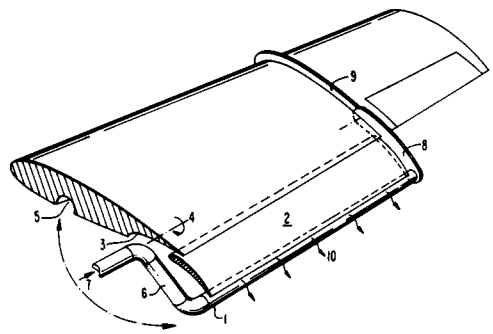

Figure 15 – Patented CC stowable rounded trailing edge in combination with Fowler flaps.

NOMENCLATURE

Ad	=	Propeller disk area
AR	=	Wing aspect ratio
b	=	Ratio of bleed air to jet engine mass flow
C_B	=	Lift proportionality constant for CC
CC	=	Circulation Controlled abbreviation
C_D	=	Total airplane drag coefficient
C_L	=	Lift coefficient
C_p	=	Coefficient of preformance for a propeller
$C\mu$	=	CC blowing coefficient
c	=	Wing chord in cruise mode
D_m	=	Engine inlet air flow momentum
e	=	Span-wise loading efficiency
f	=	Runway friction coefficient
g	=	Acceleration of gravity
h	=	Take-off obstacle height to clear or CC blowing slot height
M	=	Free stream Mach number
m	=	Mass flow rate
P_s	=	Shaft power
q	=	Free stream dynamic pressure
RC	=	Rate of Climb
S	=	Wing area in cruise
s	=	Horizontial take-off or landing distance
t	=	Temperature or time
T	=	Thrust, except with thrust vectoring is only exhaust momentum
V	=	Velocity, without subscript means flight speed
W	=	Aircraft weight
w	=	Velocity increase induced at the propeller disk

Subscripts

a	=	approach related parameter
b	=	parameter with CC blowing
c	=	climb related parameter
e	=	exhaust parameter
g	=	ground distance
i	=	induced drag
j	=	blowing jet parameter
lof	=	parameter related to lift-off speed
o	=	parasite drag or reference static thrust
T	=	thrust related parameter
w	=	head wind component
x	=	maximum angle of climb parameter

Greek

α	=	angle of attack
γ	=	flight path angle
δ_f	=	flap angle
η	=	efficiency
θ	=	thrust vector angle or flap hinge locater angle
ρ	=	air density